First and Second Concentration-Dependent Coefficients of Translational Diffusion and Sedimentation for Poly(α-methylstyrene) in a Good Solvent

Yoshisuke Tsunashima,* Taisaku Hashimoto, and Tateo Nakano

Institute for Chemical Research, Kyoto University, Uji, Kyoto 611, Japan

Received September 6, 1995; Revised Manuscript Received February 20, 1996[⊗]

ABSTRACT: The first and second concentration-dependent coefficients of translational diffusion, k_D and k_{D2}, and of sedimentation, k_s and k_{s2}, for poly(α-methylstyrene) fractions of high molecular weight in benzene at 30 °C were determined by dynamic light scattering and sedimentation velocity measurements. In the molecular weight, M_w, range of $3.76 \times 10^5 \le M_w \le 6.85 \times 10^6$, the first coefficients are positive, as reported previously, but the second are negative, which has not been previously observed. These molecular weight dependences are described by power laws ($k \propto M_w^a$), but the exponents for k_D (0.769) and k_s (0.663) and for k_{D2} (1.54) and k_{s2} (1.48) are smaller than the predicted values in the good-solvent limit, 0.80 and 1.60, respectively. Expressed in the volume-fraction frame of reference, the coefficients are not constant, which contradicts the hard sphere approximation for swollen chains, and are represented well by universal functions of X, the ratio of the thermodynamic interaction radius derived from the second virial coefficient, A_2, and the hydrodynamic chain radius derived from the diffusion coefficient; the functions are as predicted by Akcasu and Benmouna with a M_w-independent thermodynamic g factor ($=A_3/A_2^2M_w$) = 0.22−0.23. The hydrodynamic g factors defined by k_{D2}/k_D^2 and k_{s2}/k_s^2 are constant, −0.14 and −0.05, respectively, for higher M_w. The two- and three-body effective hydrodynamic interaction radii deduced from k_s and k_{s2} are larger than those from k_D and k_{D2}, indicating the long-range nature of the purely hydrodynamic interactions. The swollen chain dynamics in good solvents cannot be described by the hard sphere approximation but require a more detailed treatment of hydrodynamic interactions.

Introduction

The mutual translational diffusion coefficient, D, and the collective sedimentation coefficient, s, of a linear flexible polymer in solution depend on the polymer mass concentration, c. In the dilute solution region, the concentration dependences can be expressed by a series expansion of c as

$$D = D_0(1 + k_D c + k_{D2}c^2 + k_{D3}c^3 + ...)$$

$$s^{-1} = s_0^{-1}(1 + k_s c + k_{s2}c^2 + k_{s3}c^3 + ...) \quad (1)$$

k_D, k_{D2}, and k_{D3} are sensitive to the hydrodynamic and thermodynamic interactions of polymer chains, while k_s, k_{s2}, and k_{s3} are related only to their hydrodynamic interactions. Several attempts have been made experimentally[1−13] to determine the k_D and k_s values in good solvents; the two-body hydrodynamic interactions of polymers have been determined, e.g., for polystyrene,[1,2] polyisoprene,[3,4] poly(α-methylstyrene),[5−11] and polyisobutylene.[12,13] These data have been reviewed recently.[14] In the meanwhile, k_{D2} and k_{s2} have long been left unstudied experimentally, as well as theoretically, though these coefficients in good solvents give us information on the three-body interactions of polymers in solution. In addition, k_{D2} and k_{s2} are essential for the precise determinations of the infinite dilution values (D_0 and s_0) and the first coefficients (k_D and k_s) in a given polymer−solvent system.

Phillies was the first to predict the k_{D2} and k_{s2} values. He showed that for hard spheres the volume-fraction frame diffusion coefficient, D_ϕ, can be expressed as[15]

$$D_\phi = D_{\phi 0}(1 + 8\phi + 30\phi^2)(1 - 7.875\phi + 21.47\phi^2)$$

$$= D_{\phi 0}(1 + 0.125\phi - 11.53\phi^2 + ...) \quad (2)$$

where ϕ is the volume fraction of polymers in solution. This equation gives negative values for k_{D2} and k_{s2}, i.e., $k_{D2}^V = -11.53$ and $k_{s2}^V = -21.47$, and positive k_D and k_s values of $k_D^V = 0.125$ and $k_s^V = 7.875$. Here k_D^V, etc., which contain the superscript V, denote that these values are expressed in the volume-fraction frame, are dimensionless, and are typically expressed by

$$k_D \equiv k_D^V(N_A V_H/M_w),\ k_{D2} \equiv k_{D2}^V(N_A V_H/M_w)^2 \quad (3)$$

with V_H the hydrodynamic volume of the polymer and N_A Avogadro's number. The k_D^V and k_s^V values by Phillies are comparable to other theoretical ones for hard spheres: $k_D^V = 1.45$ and $k_s^V = 6.55$ by Batchelor[16] or $k_D^V = 0.84$ and $k_s^V = 7.16$ by Pyun and Fixman.[17] However, the experimental results so far obtained for k_D and k_s in good solvents are not satisfactorily explained by these k_D and k_s values predicted for hard spheres.

Since the second concentration-dependent coefficients have never been determined experimentally, the adequacy of Phillies' values for k_{D2} and k_{s2} has not been confirmed. Their values are only obtainable from thermodynamic data. When D is determined from dynamic light-scattering experiments at zero scattering vector ($q = 0$), D becomes the mutual diffusion coefficient which represents the relaxation of the concentration gradient in solution. Irreversible thermodynamics then yield the following relations for $D(q = 0)$ and s in the volume-fixed frame of reference:[18]

$$s/D(q = 0) = (1 - \nu_2\rho_s)^2/(\partial\Pi/\partial c)_{T,\mu_1},$$

$$s_0/D_0 = (1 - \nu_2\rho_s)^2 M/RT \quad (4)$$

[⊗] Abstract published in *Advance ACS Abstracts,* April 1, 1996.

S0024-9297(95)01319-2 CCC: $12.00

Table 1. Results Obtained from Diffusion and Sedimentation Velocity Measurements for Poly(α-methylstyrene) Fractions in Benzene at 30 °C

						triad configurations		
fraction code	M_w,[a] 10^6 g mol^{-1}	R_G,[a] 10^{-6} cm	D_0, 10^{-7} cm^2 s^{-1}	s_0, 10^{-12} s	R_H, 10^{-6} cm	I (%)	H (%)	S (%)
BB15	6.85	12.72	0.480	2.545	8.23	8	48	44
BB13	2.71	7.57	0.797	1.805	4.955	7	48	45
BB07	1.96	6.20	0.960	1.59	4.12	8	49	43
BB12	0.794	3.71	1.585	1.11	2.49	8	50	42
BB11	0.376	2.45	2.45	0.820	1.615	8	50	42

[a] Determined from static light scattering.[32]

leading to

$$D/D_0 = (s/s_0)(M/RT)(\partial\Pi/\partial c)_{T,\mu_1} \quad (5)$$

where Π is the osmotic pressure of the solution, μ_1 is the chemical potential of the solvent, M and ν_2 are the molecular weight and the partial specific volume of the polymer, respectively, ρ_s is the solvent density, and R is the gas constant. Thus, D depends on both hydrodynamic ($s/s_0 = f_0/f$) and thermodynamic [$(\partial\Pi/\partial c)_{T,\mu_1}$] interactions of polymers. Here f denotes the collective friction coefficient.

Expressing D/D_0 and s/s_0 by a series expansion of c (eq 1) and using

$$\Pi/RT = c/M + A_2c^2 + A_3c^3 + ... \quad (6)$$

we obtain from eq 5 relations which connect the concentration-dependent coefficients:[18c]

$$k_D + k_s = 2A_2M \quad (7)$$

$$k_{D2} + k_{s2} + k_Dk_s = 3A_3M \quad (8)$$

Thus, $k_{D2} + k_{s2}$ is related to A_3, as well as to k_D and k_s.

We have the following theoretical expressions for k_s by Batchelor[16](Ba), Felderhof[19](Fe), Pyun and Fixman[17](PF), and Akcasu and Benmouna[20,21](AB):

$$k_s = BN_AV_H/M \text{ (Ba, Fe, PF)}$$

$$k_s = (6/4^{2/3})(A_2M)^{2/3}(N_AV_H/M)^{1/3} \text{ (AB)} \quad (9)$$

In the good-solvent limit, it is assumed that interactions between polymers behave as those between effective hard spheres of radius R_a and the particle volume $V_e = V_H = (4\pi/3)R_a^3$ and that $A_2M = 4N_AV_e/M = 4N_AV_H/M$. We then obtain from eqs 7 and 9 the relations:

$$k_D = (2 - B/4)A_2M,\ k_s = (B/4)A_2M \text{ (Ba, Fe, PF; hard spheres)}$$

$$k_D = (1/2)A_2M,\ k_s = (3/2)A_2M \text{ (AB; hard spheres)} \quad (10)$$

with $B = 6.55$ (Ba), 6.44 (Fe), and 7.16 (PF). Substitution of eq 10 into eq 8 gives a rough prediction for the molecular weight dependence of $k_{D2} + k_{s2}$ in the good-solvent limit (=hard spheres): $k_{D2} + k_{s2} = 3A_3M - \beta(A_2M)^2$, with β a constant. Considering experimental asymptotes $A_2 \propto M^{-0.2}$ and $A_3 \propto M^{0.6}$ attained at large M, which have been reported for polystyrene in benzene[22,23] and toluene,[24] we may predict that $k_{D2} + k_{s2}$ will be proportional to $M^{1.6}$. In addition, the ratios such as k_D/k_s and k_{D2}/k_D^2, the latter representing the hydrodynamic interaction g factor $g_D \equiv k_{D2}/k_D^2$ as opposed to the so-called g (=A_3/A_2^2M) factor for the thermodynamic interactions of polymers, is predicted to be independent of M, though the absolute values are not obvious.

In this article, we made dynamic light-scattering and sedimentation velocity measurements on solutions of narrow molecular weight distribution poly(α-methylstyrene) samples of higher molecular weight in benzene at 30 °C. The first and second concentration-dependent coefficients were determined by using a *finite difference method*. The results obtained are discussed in terms of the hydrodynamic interactions of polymers.

Experimental Section

Samples. Five poly(α-methylstyrene) samples (designated PαMS) with narrow molecular weight distribution were prepared by anionic polymerization at −78 °C in tetrahydrofuran, using *n*-butyllithium as the initiator and *n*-butyl alcohol as the terminator.[25] Each sample was purified several times by dissolution in benzene and precipitation into methanol and divided into three parts by successive solution column fractionation using benzene as the solvent and ethanol as the precipitant. In the fractionation for each sample, the central fraction, excepting the first and last elutes of about 10% and 3% of the material, respectively, was collected and freeze-dried from a filtered benzene solution. These samples were sealed into ampules at 10^{-6} mmHg and stored in the refrigerator just prior to use. They were designated as BB07, BB11, BB12, BB13, and BB15. The weight-average molecular weight, M_w, ranging from 3.76×10^5 to 6.85×10^6, and the M_w/M_n values determined previously[25] were checked again by GPC with a low-angle light-scattering apparatus (Tosoh HLC-802UR/LS-8); the M_w values were in agreement with the previous ones to within ±1% with M_w/M_n well below 1.05 for five samples. The results are listed in Table 1.

The stereospecific configuration of the samples was determined from the NMR spectra on α-methyl resonances and expressed in terms of triad configurations: isotactic (I), heterotactic (H), and syndiotactic (S); three α-methyl resonances at about 9.0, 9.4, and 9.7 ppm measured at 100 MHz (Varian) in chlorobenzene at 120 °C were assigned to I, H, and S with increasing field strength. As summarized in Table 1, the triad configuration was, in all samples, 7−8% I, 48−50% H, and 42−45% S.

Dynamic Light Scattering. Measurements of the time correlation function, $A(t)$, were made on a laboratory-made time-interval correlator (512 channels with linear time scale)[26] using the vertically polarized incident light of a single-frequency 488 nm line emitted from an etalon-equipped Ar ion laser (3W, Spectra Physics). The vertically polarized scattered light from the solution of a given concentration c was determined by the homodyne method at six fixed angles, θ, in the range from 10° to 150° at 30.00 ± 0.02 °C. The accumulation of $A(t)$ data at given c and θ was made for more than 1 h; this process ascertains that errors were <3% in the determination of the decay rates of $A(t)$ (see data analyses).

The apparatus was calibrated at 30 °C by using pure benzene and a 10^{-5} (g/g) aqueous solution of polystyrene (PS)−latex particles of uniform diameter (d = 0.091 μm; Dow Chemical). Benzene did not show any decay feature in the $A(t)$ measured at the time in the range from 0.4 μs to 1.5×10^5 μs and at θ in the range of 10° to 150°. For the PS−latex aqueous solution, the normalized time correlation function was a single-exponential decay curve, $A(t) = \beta|\exp(-\bar{\Gamma}t)|^2 + 1 + \Delta$,

with the *z*-average normalized variance $\mu_2/\bar{\Gamma}^2 < 0.005$, the baseline uncertainty $|\Delta| \leq \pm 0.003$, and the frequency $\beta > 0.7$. Here $\bar{\Gamma}$ is the mean decay rate, and μ_2 is the second moment of the decay rate Γ about the mean $\bar{\Gamma}$, i.e., $\mu_2 = \int_0^\infty (\Gamma - \bar{\Gamma})^2 G(\Gamma)\, d\Gamma$, with $G(\Gamma)$ the distribution function of Γ. At all θ measured, $\bar{\Gamma}/\sin^2(\theta/2)$, which corresponds to the translational diffusion coefficient of the PS−latex particle, gave a constant value, $\bar{\Gamma}/\sin^2(\theta/2) = k_B T/\{[6\pi\eta_s(d/2)](4\pi n_0/\lambda_0)^2\} = 7201\ s^{-1}$, to within ±1%. For benzene at 30 °C, the viscosity, η_s, was 5.62×10^{-3} g cm^{-1} s^{-1} and the refractive index, n_0, was 1.5060 for light of wavelength $\lambda_0 = 488$ nm.

Polymer solutions of eight to nine concentrations were prepared for each sample. To do this, benzene solutions with concentration of ca. 50% and 80% of the critical overlap concentration, c^*, were prepared and stored overnight at 40 °C with gentle stirring. A suitable amount of this solution and benzene were filtered directly into specially prepared precision light-scattering cells through Millipore filters of 0.2 μm pore size. Prior to use, the cells were optically cleaned by a reflux method. The polymer mass concentration, c, in each solution was calculated from the weight fraction of the solute assuming that the solution density was equal to the solvent density.

Sedimentation Velocity. Sedimentation velocity measurements were made on an analytical ultracentrifuge (Beckman, Spinco Model E) with a light of *e* line from Hg (546 nm) at 30.0 ± 0.1 °C. A single-sector 12 mm cell was used at a rotor speed of 40 000 rpm. Schlieren diagrams were read on a contour projector (Nihon Kogaku, L-16) to the accuracy of 0.001 mm. Polymer solutions of eight to nine concentrations were prepared for each sample using the same procedures as for DLS measurements, except for optical cleaning of the solutions by Millipore filters. The solvent density, ρ_s, and the partial specific volume of the polymer at infinite dilution, ν_2, were 0.8685 g cm^{-3} and 0.883 cm^3 g^{-1},[9] respectively, at 30 °C.

Data Analyses and Evluation of Infinite Dilution Values. Dynamic Light Scattering. The $A(t)$ curve measured at finite c and θ was analyzed by the histogram method, whose validity has already been demonstrated.[27] At $qR_G > 1$, with q the scattering vector and R_G the radius of gyration of the polymer, the distribution function of decay rate Γ, $G(\Gamma)$, was expressed by two well-separated peaks. The component with low decay rates, i.e., the slow component, was assigned to the translational diffusion mode when the mean value Γ_{slow} divided by $\sin^2(\theta/2)$ was constant in the range of $\theta = 10-150°$. Here Γ_{slow} was estimated by averaging Γ with the $G(\Gamma)$ over the slow component only. The diffusion coefficient for solution of a given c was thus calculated from Γ_{slow}. This D value was in good agreement with D estimated from $A(t)$ at smaller θ where the condition $qR_G \ll 1$ was satisfied. In the qR_G region of $qR_G \ll 1$, D is theoretically given by $D \equiv [\Omega(q)/q^2]_{q\to 0}$, with Ω the first cumulant. In the histogram method, Ω is given by the effective decay rate, Γ_e, which is defined by $\Gamma_e \equiv \int_0^\infty \Gamma G(\Gamma)\, d\Gamma$. At $qR_G \ll 1$, $A(t)$ data were well fitted by single-exponential decay, and the histogram analysis of the $A(t)$ data gave a sharp unimodal Γ distribution, as typically realized at $\theta = 10°$ for all $A(t)$ data measured. This enabled us to determine the translational diffusion coefficient to within ±2−3% even when $A(t)$ of the highest molecular weight sample (BB15) at $\theta = 10°$ was analyzed with a unimodal Γ distribution, where $qR_G = 0.430$.

The D values thus obtained at finite c, $D(c)$, as expressed by eq 1, were analyzed by using the following "difference expression", originally derived by Bawn et al.:[28]

$$S_D(c_i,c_j) \equiv [D(c_i) - D(c_j)]/(c_i - c_j) = D_0 k_D + D_0 k_{D2}(c_i + c_j) + D_0 k_{D3}(c_i^2 + c_i c_j + c_j^2) + \ldots \quad (11)$$

where c_i and c_j are the different mass concentrations of solutions for a given sample. The intercept and the initial slope of a plot of $S_D(c_i,c_j)$ vs $c_i + c_j$ for each sample gave $D_0 k_D$ ($\equiv K_1$) and $D_0 k_{D2}$ ($\equiv K_2$), respectively, for the sample. With K_1 and K_2 thus obtained, an apparent translational diffusion coefficient at infinite dilution, $D_{0,app}$, defined from eq 1 by

$$D_{0,app} = D(c_i) - K_1 c_i - K_2 c_i^2 \quad (12)$$

was calculated at $c = c_i$. The extrapolation of $D_{0,app}$ to $c = 0$ gave the true D_0 value for each sample. The k_D and k_{D2} values were then estimated from

$$k_D = K_1/D_0,\ k_{D2} = K_2/D_0 \quad (13)$$

Sedimentation Velocity. The position of the sedimentation boundary, r, was determined from the maximum of the refractive index gradient on the Schlieren diagram. The sedimentation coefficients at finite polymer concentration, $s(c)$, were estimated by fitting the movement of r to the Billick−Fujita equation:

$$\ln(r/r_m)/\omega^2(t - t_0) = s(c)\{1 + B[(r/r_m)^2 - 1]\} \quad (14)$$

which takes account of the zero-time and the pressure-effect corrections in the experimental system. Here r and r_m denote the radial distances of the sedimentation boundary and the meniscus from the rotor axis, respectively, ω is the angular velocity, t is the time measured from the moment when the rotor is set in motion, and B is a constant relating to the pressure effect on $s(c)$. The value of the zero-time correction for the acceleration period, t_0, was chosen so that plots of $\ln(r/r_m)/\omega^2(t - t_0)$ vs $(r/r_m)^2 - 1$ became linear over the total range of the abscissa (Blair and Williams method[29]). The correct $s(c)$ was obtained from the intercept of the plot. In this procedure, various t_0 values were tested around the first-approximation t_0 value which minimizes approximately the mean square deviation, Δ^2, defined by

$$\Delta^2 \equiv (1/n)\sum_{i=1}^{n} [s(c)\omega^2(t_i - t_0)\{1 + B[(r/r_m)^2 - 1]\} - \ln(r/r_m)]^2 \quad (15)$$

where t_i is the time when the Schlieren diagram was observed and n is the number of the observation ($i = 1-n$).

When $s(c)$ is expressed by eq 1, the "difference expression" is given as

$$S_s(c_i,c_j) \equiv [s^{-1}(c_i) - s^{-1}(c_j)]/(c_i - c_j) = k_s/s_0 + (k_{s2}/s_0)(c_i + c_j) + (k_{s3}/s_0)(c_i^2 + c_i c_j + c_j^2) + \ldots \quad (16)$$

With the same procedures as in DLS data analyses, k_s/s_0 ($\equiv K_3$) and k_{s2}/s_0 ($\equiv K_4$) were obtained from the intercept and the initial slope of a plot of $S_s(c_i,c_j)$ vs $c_i + c_j$, respectively, for each sample. The apparent sedimentation coefficient at infinite dilution, $s_{0,app}$, defined by $s_{0,app} = s^{-1}(c_i) - K_3 c_i - K_4 c_i^2$, was calculated at $c = c_i$. The true s_0 value for each sample was estimated from the extrapolation of $s_{0,app}$ to $c = 0$. k_s and k_{s2} were then given by $k_s = K_3 s_0$ and $k_{s2} = K_4 s_0$, respectively.

Results

Diffusion. Figure 1 demonstates DLS results for the highest molecular weight sample, BB15. In Figure 1A, the diffusion coefficient at finite concentration, $D(c)$, is plotted against the polymer concentration, c. $D(c)$ increases with c and can be fitted to an upward-convex curve, indicating positive k_D and negative k_{D2}. The Bawn plot using these $D(c)$ values, $S_D(c_i,c_j)$ vs $c_i + c_j$ plot, is shown in Figure 1B. The 28 plotted points fall on a straight line with a negative slope over the $c_i + c_j$ region measured and ensure a definite determination of $D_0 k_D$ and $D_0 k_{D2}$. The contribution of k_{D3} is negligible in the range of concentrations used. The apparent diffusion coefficient, $D_{0,app}$, calculated with the $D_0 k_D$ and

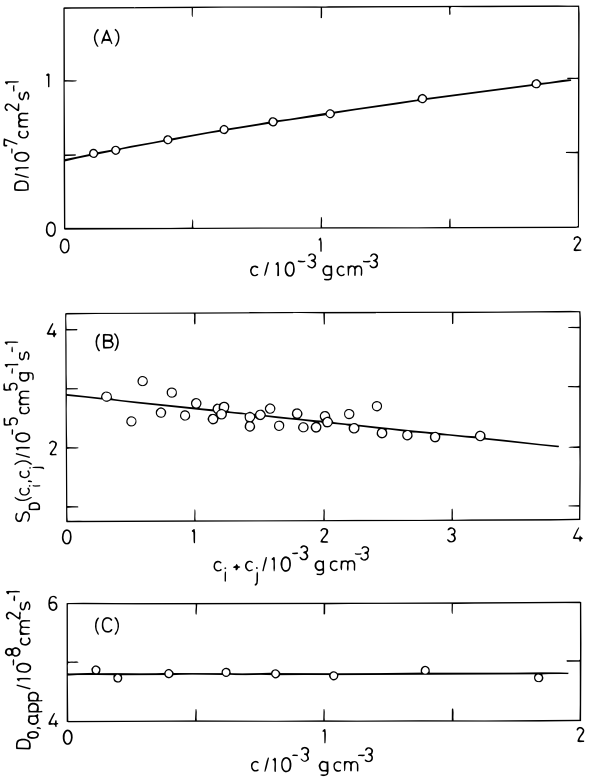

Figure 1. Concentration dependence of diffusion coefficients, D, for a poly(α-methylstyrene) fraction (BB15) in benzene at 30 °C: (A) plot of $D(c)$ against the polymer mass concentration, c, (B) Bawn plot, and (C) plot of the apparent diffusion coefficient at infinite dilution, $D_{0,app}$, against c.

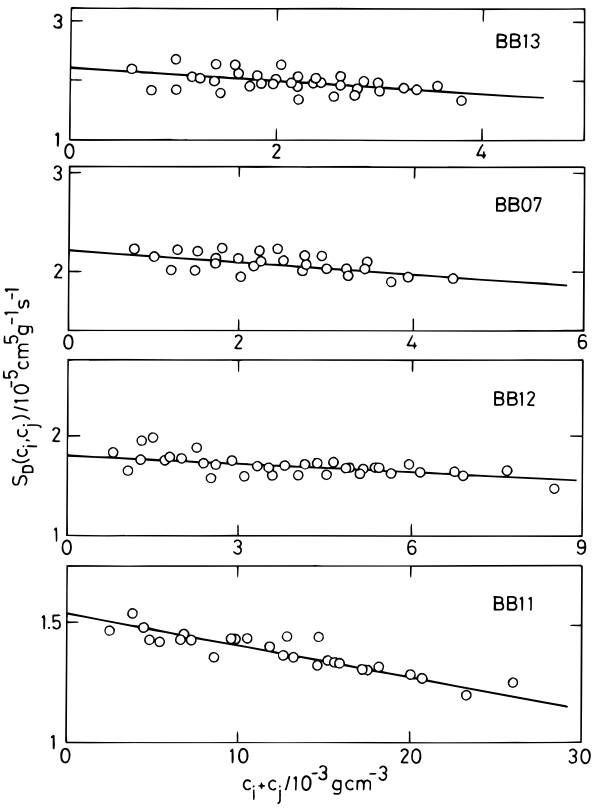

Figure 2. Bawn plots for the indicated poly(α-methylstyrene) fractions in benzene at 30 °C.

D_0k_{D2} values at a given c_i is plotted against c in Figure 1C. The points are well represented by a horizontal line, which gives D_0 as the average of these $D_{0,app}$ and offers k_D and k_{D2} from eq 13.

Bawn plots for the others, i.e., BB13, BB07, BB12, and BB11, are shown in Figure 2. The plots of 28 or 36 points of each sample are linear with a negative slope, which yields positive k_D and negative k_{D2}, as in the case for BB15. The D_0, k_D, and k_{D2} values estimated are summarized in Tables 1 and 2.

Sedimentation. Figure 3 illustrates the results of sedimentation velocity experiments for the second highest molecular weight sample, BB13. In Figure 3A, the determination of the zero-time correction, t_0, is demonstrated for a solution of $c = 1.966 \times 10^{-3}$ g cm^{-3} by plotting $\ln(r/r_m)/\omega^2(t - t_0)$ as a function of $(r/r_m)^2 - 1$. For the assumed four t_0 values, the mean square-fitting deviation, Δ^2, is shown in the insert, and the best-fit t_0 value of $t_0 = 327$ s (the filled circles) results in a straight line in the $\ln(r/r_m)/\omega^2(t - t_0)$ vs $(r/r_m)^2 - 1$ plots, the intercept giving the true $s(c)$ value. Figure 3B shows the plot of $s^{-1}(c)$ estimated as a function of c for BB13; $s^{-1}(c)$ increases but the increment decreases with increasing c.

Bawn plots for this sample and the others, $S_s(c_i + c_j)$ vs $c_i + c_j$ plots, are shown in Figure 4. The plots of 28 or 36 points for each sample are linear with a negative slope over the entire $c_i + c_j$ range and give the accurate k_s/s_0 (positive) and k_{s2}/s_0 (negative) values for each sample. The contribution of k_{s3} is again negligible. With these k_s/s_0 and k_{s2}/s_0 values, the apparent sedimentation coefficient, $s_{0,app}$, for each sample was calculated at different c and found to be independent of c. For each sample, s_0 was determined as the average of these $s_{0,app}$, and then k_s and k_{s2} were estimated from this s_0. The s_0, k_s, and k_{s2} values thus obtained are summarized in Tables 1 and 2. Over the range of M_w studied, k_{s2} is negative as in the case for k_{D2}.

It has recently been suggested that in Bawn plots the second concentration-dependent coefficients are estimated successfully in the appropriate ranges of concentration, and the values are confirmed by polynomial

Table 2. First and Second Concentration-Dependent Coefficients for Poly(α-methylstyrene) Fractions in Benzene at 30 °C

fraction code	k_D, cm^3 g^{-1}	k_s, cm^3 g^{-1}	k_{D2}, cm^6 g^{-2}	k_{s2}, cm^6 g^{-2}	k_D^V	k_s^V	k_{D2}^V	k_{s2}^V
BB15	598	1310	−47 650	−80 750	2.91	6.39	−1.13	−1.92
			(−48 500)[a]	(−83 800)				
BB13	280	727	−12 600	−26 800	2.48	6.42	−0.983	−2.09
			(−12 000)	(−25 900)				
BB07	231	588	−6390	−15 850	2.575	6.55	−0.793	−1.97
			(−6810)	(−15 800)				
BB12	114	316	−1750	−3890	2.315	6.43	−0.722	−1.61
			(−1780)	(−3890)				
BB11	63.3	193	−553	−1150	2.245	6.84	−0.695	−1.445
			(−596)	(−1070)				

[a] The values in parentheses were estimated by the polynomial regressions.

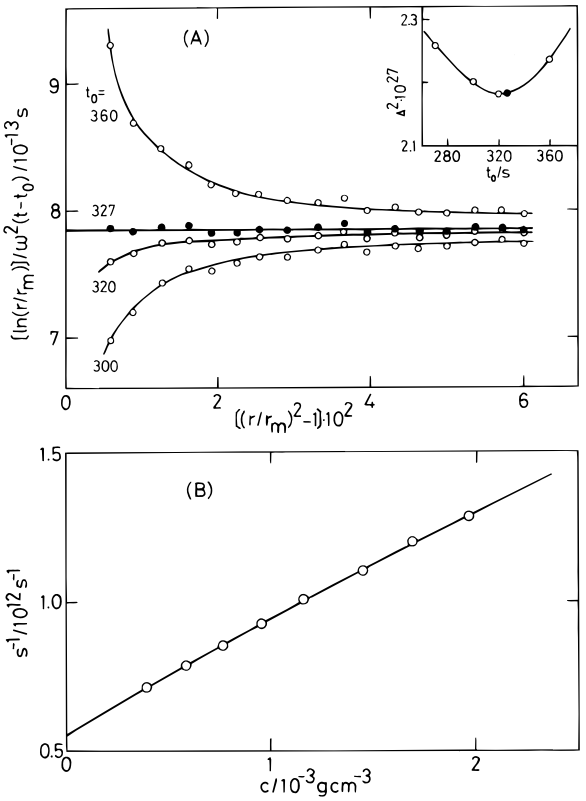

Figure 3. Sedimentation velocity results for a poly(α-methylstyrene) fraction (BB13) in benzene at 30 °C. (A) Determination of the zero-time correction, t_0, by plotting the apparent sedimentation coefficient $\ln(r/r_m)/\omega^2(t - t_0)$ against $(r/r_m)^2 - 1$ with four different t_0 values. The insert shows variation of the mean square deviation, Δ^2, with the assumed five values at t_0; $c = 1.966 \times 10^{-3}$ g cm^{-3}. (B) Concentration dependence of sedimentation coefficients, $s(c)$.

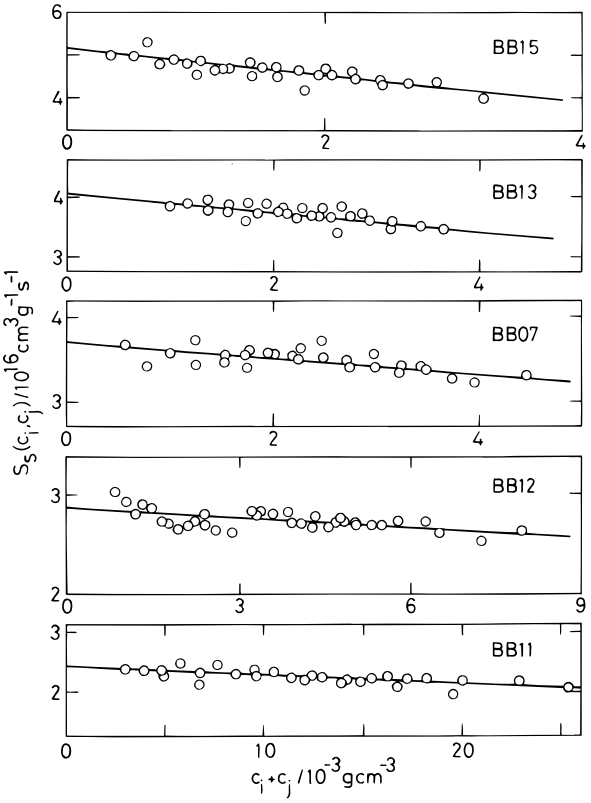

Figure 4. Bawn plots on sedimentation coefficients for the indicated poly(α-methylstyrene) fractions in benzene at 30 °C.

regressions.[30] In Table 2, the k_{D2} and k_{s2} values from polynomial regressions are shown in parentheses. Bawn plots and polynomial regressions give k_{D2} and k_{s2} agreeing to within ±7%.

Discussions

Diffusion and Sedimentation Coefficients. Figure 5 shows a plot of the present D_0 data in benzene at 30 °C against M_w. The data points shown by unfilled circles are well fitted by

$$D_0 = 3.26 \times 10^{-4} M_w^{-0.561} \text{ (cm}^2 \text{ s}^{-1}\text{)} \qquad (17)$$

In the same figure, D_0 data for PαMS of M_w lower than ours are also shown, including data in toluene at 25 °C by Lindner et al.[5] and data in benzene at 30 °C and toluene at 25 °C by Selser et al.[6,8] These data also agree with eq 17. Thus, for PαMS in good solvents, $D_0 \propto M_w^{-0.561}$ holds in the range of M_w from 10^4 to 10^7, though the sample tacticity may vary for $M_w < 2 \times 10^5$.[31] The exponent of $\nu_D = -0.561$ lies below the asymptotic value, −0.60, predicted for linear flexible polymers in good solvents. The value −0.60 was found in the rubbery polymer−good-solvent system of polyisoprene in cyclohexane at 25 °C.[3] The low value of ν_D in the present system is similar as for polystyrene in good solvents, $\nu_D \simeq -0.55$.[1] It is interesting that the value −0.6 has recently been reported for polyisobutylene in chloroform at 25 °C.[12]

Calculating the hydrodynamic radius, R_H, for each sample from the Stokes−Einstein relation $R_H = k_BT/6\pi\eta_s D_0$ (R_H representation of eq 17 is $R_H = 1.215 \times 10^{-9} M_w^{0.561}$) and using the corresponding R_G value, which will be reported in the forthcoming paper,[32] we obtain the radius ratio $R_G/R_H = 1.49-1.55$ for the PαMS/benzene system, with the value slightly increasing with M_w. This value is consistent with those established experimentally for highly swollen flexible chains in good solvents: 1.54 (PαMS/toluene),[5] 1.50[3] or 1.38−1.45[4] (polyisoprene/cyclohexane), 1.41−1.63 (PS/benzene),[1] and 1.35−1.61 (PS/THF, ethylbenzene),[33] but is much smaller than the theoretical value for pseudo-Gaussian swollen chains, 1.860.[34,35] Reasons for the differences between experiment and theory were attributed by us[3,35] to the non-Gaussian nature in the swollen chain segment distributions and to the Oseen

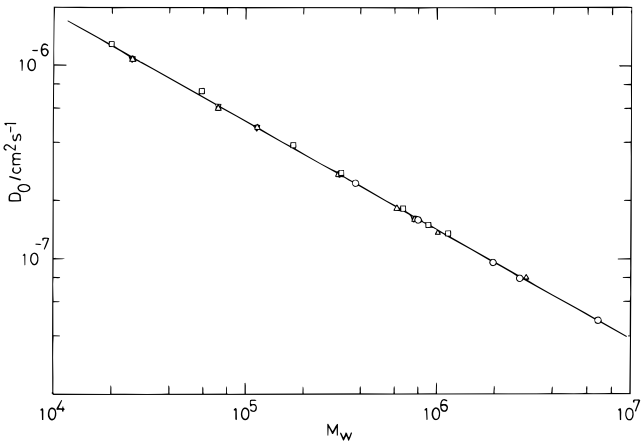

Figure 5. Molecular weight dependence of diffusion coefficients at infinite dilution, D_0, for poly(α-methylstyrene): (○) present work in benzene at 30 °C, (□) data by Lindner et al. in toluene at 25 °C,[5] (△) data by Selser et al. in toluene at 25 °C,[6,8] and (▽) data by Selser in benzene at 30 °C.[6] The solid line represents eq 17.

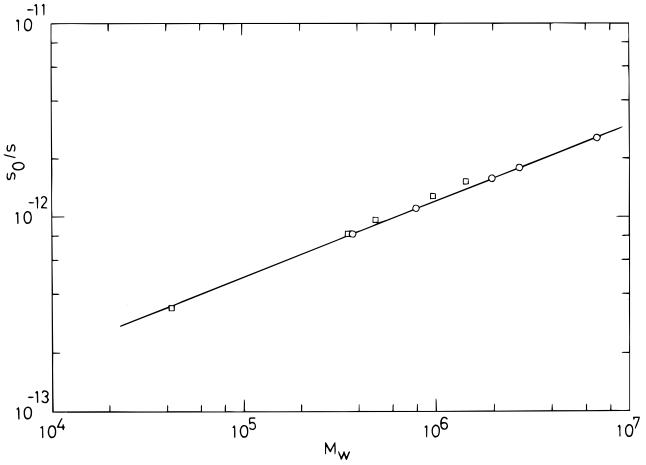

Figure 6. Molecular weight dependence of sedimentation coefficients at infinite dilution, s_0, for poly(α-methylstyrene) in benzene at 30 °C: (○) present work and (□) data by Sakato and Kurata.[9] The solid line represents eq 18.

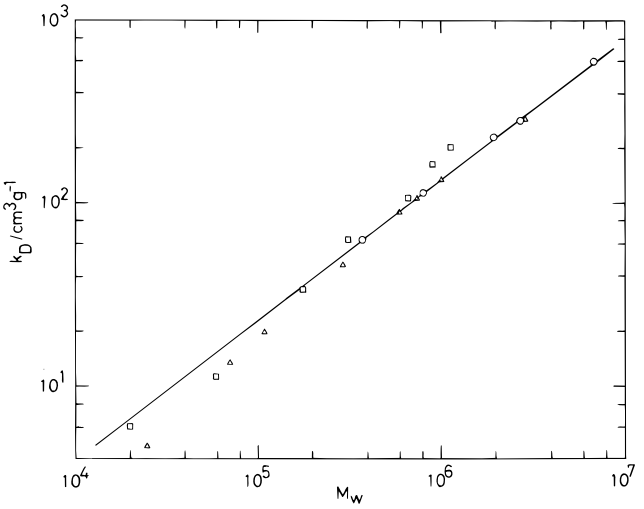

Figure 7. Molecular weight dependence of k_D for poly(α-methylstyrene): (○) present work in benzene at 30 °C, (□) data by Lindner et al. in toluene at 25 °C,[5] and (△) data by Selser et al. in toluene at 25 °C.[6,8] The solid line represents eq 19.

hydrodynamic interactions in the Kirkwood scheme; the R_G/R_H value for fully swollen chains was reasonably predicted to be 1.596 with the chain expansion parameters $\nu = 0.5830$, $t = 2.398$, and $l = 2.802$. Since Gaussian chains should have $t = l = 2$, this discussion suggests that R_G/R_H is affected by a variation in internal friction with chain expansion. Another attempt to explain the discrepancy has recently been made by Shiwa and Tsunashima[36,37] using a couple of kinetic model equations for polymer and solvent. Here the polymer−solvent coupling expressed by the ratio of the solvent viscosity in the bulk, η_s, to that in the neighborhood of the polymer (the local viscosity), η_e, i.e., η_s/η_e, affected R_G/R_H, and the relation $R_G/R_H = 0.3920\eta_s/\eta_e$ held for self-avioding chains in the nondraining limit. The parameter η_s/η_e, when redefined by a dimensionless parameter, λ_0, as $\lambda_0^2 \equiv \eta_s/\eta_e$, was nearly constant with $\lambda_0 \simeq 2.0$, irrespective of the species of polymers and for both good and Θ solvents. Very recently, Douglas and Freed[38] have presented a polymer droplet model and predicted that R_G/R_H ranges from 1 to 1.5 as a parameter representing the measure of the chain mobility relative to that of solvent changes from 0 to infinity. The upper end of this R_G/R_H value, however, can never explain the experimental values which exceed 1.5, as described above.

Figure 6 shows the plot of the present s_0 data (unfilled circles) as a function of M_w, together with data in benzene at 30 °C by Sakato and Kurata.[9] The straight solid line in the figure is the best-fit line to the present data, expressed as

$$s_0 = 5.46 \times 10^{-15} M_w^{0.391} \text{ (s)} \qquad (18)$$

The line fits all points plotted for M_w from 4×10^4 to 10^7.[39] The exponent of M_w, $\nu_s = 0.391$, is slightly smaller than 0.40, the asymptotic value for the linear flexible polymers in good solvents. Comparing the ν_s and ν_D values in eqs 18 and 17, we find that the approach of ν_s to its good-solvent limit value, $\nu_{s,\infty} = 0.40$, is much faster than that of ν_D to $\nu_{D,\infty} = -0.60$ for PαMS in benzene. This difference in ν might be a reflection of distinct features between k_D (k_{D2}) and k_s (k_{s2}) described in the following sections.

First Concentration-Dependent Coefficients. Figure 7 gives a plot of the present k_D data in benzene at 30 °C (unfilled circles) against M_w, together with data in toluene at 25 °C by Lindner et al.[5] and Selser et al.[6,8] Our data for $3.76 \times 10^5 < M_w < 6.85 \times 10^6$ fall on a straight line, represented by

$$k_D = 3.28 \times 10^{-3} M_w^{0.769} \text{ (cm}^3 \text{ g}^{-1}) \qquad (19)$$

The slope of 0.769 is smaller than 0.80, the good-solvent limit value predicted from $k_D \propto A_2 M_w$ (eq 10) with $A_2 \propto M_w^{-0.20}$ under the hard sphere approximation. In addition, the solid line in the figure seems to stand for approximately a part of Lindner et al.'s data which are located in the limited range of M_w for $2 \times 10^4 < M_w < 7 \times 10^5$. Their data points for $M_w > 9 \times 10^5$, however, are fairly above the solid line and, if combined with their data for $M_w < 9 \times 10^5$, lead to $k_D \propto M_w^{0.9}$ with its strangely large exponent. The same exponent is obtained for $M_w \leq 10^5$ by Selser et al.[6,8]

k_D represents the two-body hydrodynamic and thermodynamic interactions of polymers in a given solvent and at a given temperature. It is usually characterized by the ratio X, defined by S_T/R_H,[20,21] with S_T the thermodynamic two-body interaction radius. Here S_T is introduced as an effective radius which is related to the second-virial coefficient by

$$A_2 M_w = 4(4\pi/3) N_A S_T^3 / M_w \qquad (20)$$

X represents, therefore, the excluded-volume effect normalized by the hydrodynamic chain radius. It can also be expressed by $X = (3\pi^{1/2}/4)^{1/3} \Psi^{1/3} (R_G/R_H)$, with Ψ the interpenetration function. In the good-solvent limit, if the chain behaves approximately as a hard sphere, X should be 1.0 because $S_T = R_H$. Figure 8A shows, by unfilled circles, the molecular weight dependence of X for the present system. For $3.76 \times 10^5 < M_w < 6.85 \times 10^6$, X is always larger than unity and increases with increasing M_w, reaching 1.07 at $M_w = 10^7$. Similar behavior in X is also demonstrated by the Lindner et al.'s data (squares) in the same figure.

A value of X larger than unity indicates that the hard sphere approximation is inadequate for the representation of well-swollen chains in good solvents and that the thermodynamic two-body interactions act over a range longer than the hydrodynamic polymer size, R_H. Using R_H, we can change k_D into the dimensionless or the

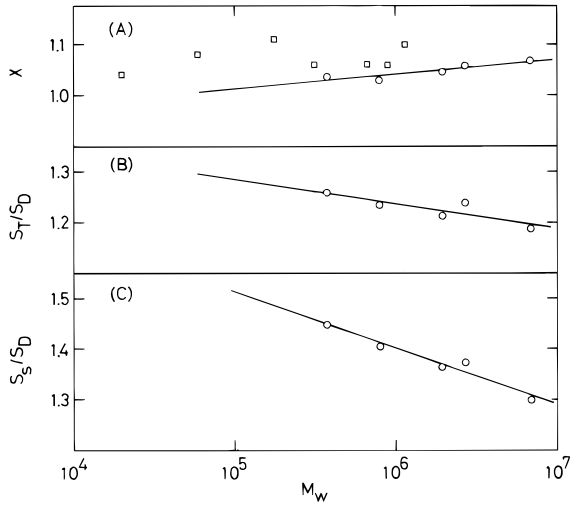

Figure 8. Molecular weight dependence of the two-body interaction radius, S_T, S_D, and S_s, for poly(α-methylstyrene): (○) present work in benzene at 30 °C and (□) data by Lindner et al. in toluene at 25 °C.[5] (A) X, defined by the ratio of the effective A_2 radius S_T to the Stokes radius R_H, plotted against M_w. (B) Ratio of S_D, the effective k_D radius, to S_T plotted against M_w. (C) Ratio of S_s, the effective k_s radius, to S_D plotted against M_w.

volume-fraction frame value k_D^V, which is written from eq 3 as

$$k_D \equiv k_D^V(4\pi N_A R_H^3/3M_w) \tag{21}$$

The k_D^V values thus estimated for the present data are summarized in Table 2 and plotted against X in Figure 9 (filled circles). k_D^V increases with an increasing solvent power. The behavior is well represented by the theoretical curve AB given by Akcasu and Benmouna,[21] $k_D^V = X^2(8X - 6)$ ($X > 0$), not the curve PF by Pyun and Fixman (a modified expression by Akcasu and Benmouna),[21] $k_D^V = 8X^3 - B(X)$. Here $B(X)$ is a function of X.[21] In the figure the data for polyisoprene,[3,4] polystyrene,[1,2] PαMS,[5,8] and polyisobutylene[13] are also shown, located around the AB curve. Several k_D^V values have been predicted theoretically for hard spheres: 1.54 (Batchelor[16]), 0.84 (original Pyun−Fixman[17]), and 0.125 (Phillies[15]) at $X = 1.0$. These are located below the AB line and can never explain the experimental data.

We can also express k_D in terms of the hydrodynamic two-body interaction radius, S_D, defined, by analogy with the thermodynamic interaction radius, S_T, in eq 20, by

$$S_D \equiv \{[4(4\pi N_A/3)]^{-1}k_D M_w\}^{1/3} \tag{22}$$

Hereafter, we call S_D and S_T the effective k_D and the effective A_2 radius, respectively. With the help of Table 3 where S_D for the present system is given, the ratio of the two-body interaction radii, S_T/S_D, is plotted against M_w in Figure 8B. It assumes at $M_w = 10^7$ a value of ca. 1.2, which is larger than X and then increases with a decreasing M_w. This means that the hydrodynamic interaction distance represented by S_D is much shorter than the thermodynamic one and that the former becomes shorter at lower M_w. Thus the hard sphere approximation of swollen chains fails again.

The present k_s data are plotted against M_w in Figure 10 (unfilled circles), together with previous PαMS data

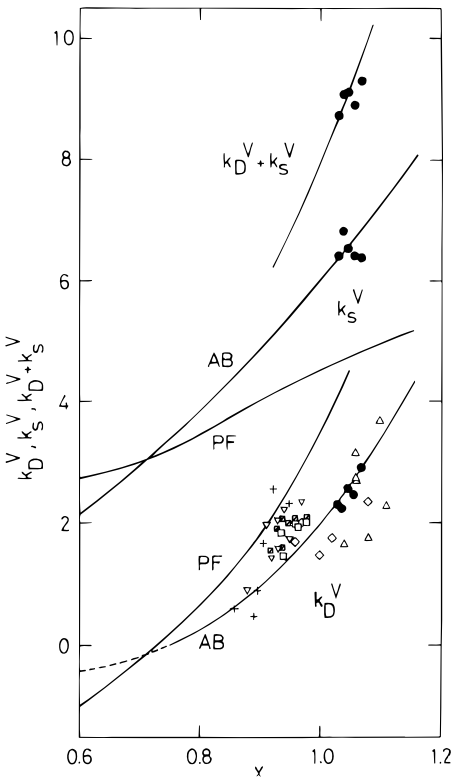

Figure 9. Variation of the volume-fraction frame k_D and k_s values, i.e., k_D^V and k_s^V, with X for poly(α-methylstyrene): (●) present work in benzene at 30 °C, (△) data by Lindner et al. in toluene at 25 °C,[5] (▽) data by Cotts and Selser in toluene at 25 °C,[8] (◇) data by Tsunashima et al. in benzene at 30 °C for polystyrene,[1,2] (□) data by Tsunashima et al. in cyclohexane at 25 °C for polyisoprene,[3] (⧄) data by Davidson et al. in cyclohexane at 25 °C for polyisoprene,[4] and (+) data by Fetters et al. in cyclohexane and *n*-heptane at 25 °C for polyisobutylene.[13] The solid lines AB and PF are the theoretical curves by Akcasu and Benmouna[20,21] and Pyun and Fixman (a modified form by Akcasu and Benmouna),[21] respectively. For further details, see the text.

by Sakato-Kurata[9] and Noda et al.[10] Our data are fitted by

$$k_s = 3.88 \times 10^{-2} M_w^{0.663}\ (\mathrm{cm^3\ g^{-1}}) \tag{23}$$

This fits also previous data for $M_w > 3 \times 10^5$. The slope of 0.663, however, is much smaller than 0.8, the asymptotic good-solvent value for hard spheres. The deviation of the previous data from the solid line for $M_w < 5 \times 10^5$ might be related to variation in the sample tacticity with M_w for $M_w < 2 \times 10^5$.[31] The volume-fraction frame k_s values, k_s^V, calculated by $k_s^V = k_s(4\pi N_A R_H^3/3M_w)^{-1}$, for the present data are plotted against X in Figure 9.[40] The points are located around the theoretical curve AB by Akcasu and Benmouna,[20,21] $k_s^V = 6X^2$, which gives 6.62 at $X = 1.05$, but not on the curve PF by Pyun and Fixman, $k_s^V = B(X)$.[21] It is interesting to note that the plotted k_s^V values are accidentally very close to the hard sphere ($X = 1$) value 6.55 by Batchelor[16] but far below 7.875 by Phillies.[15]

In Figure 9, the $k_D^V + k_s^V$ values are also plotted against X for the present data. They fall on the solid curve consistent with $k_D^V + k_s^V = 8X^3$. This agrees with $k_D + k_s = 2A_2M_w$ (eq 7); the Gibbs−Duhem relation holds for k_D and k_s.

The pure hydrodynamic two-body interaction radius, S_s, defined as for S_D and called the k_s radius, was estimated from $S_s = [(16\pi N_A/3)^{-1}k_s M_w]^{1/3}$ for the present

Table 3. Effective Radii of the Two-Body and Three-Body Hydrodynamic Interactions and Hydrodynamic *g* Factors for Poly(α-methylstyrene) Fractions in Benzene at 30 °C

fraction code	S_D, 10^{-6} cm	S_s, 10^{-6} cm	S_{D2}, 10^{-6} cm	S_{s2}, 10^{-6} cm	$X = S_T/R_H$[a]	g_D	g_s
BB15	7.40	9.62	−5.29	−5.78	1.07	−0.133	−0.0470
BB13	4.22	5.80	−3.11	−3.53	1.06	−0.160	−0.0507
BB07	3.55	4.85	−2.495	−2.90	1.045	−0.120	−0.0459
BB12	2.08	2.92	−1.49	−1.70	1.03	−0.135	−0.0389
BB11	1.33	1.93	−0.957	−1.08	1.04	−0.138	−0.0309

[a] S_T was calculated from A_2.[32]

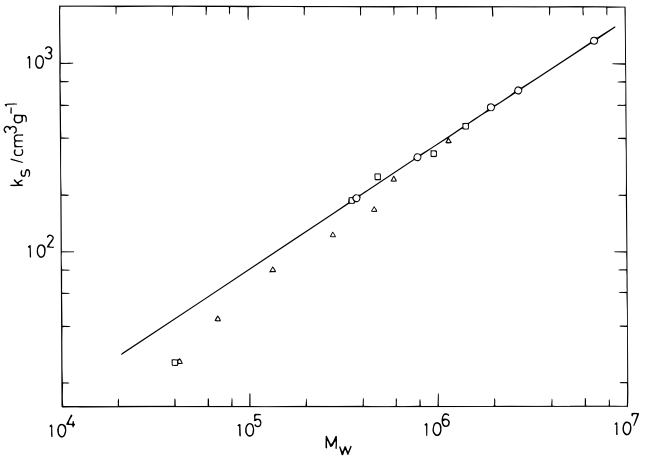

Figure 10. Molecular weight dependence of k_s for poly(α-methylstyrene): (○) present data, (□) data by Sakato and Kurata,[9] and (△) data by Noda et al. in toluene at 25 °C.[10] The solid line represents eq 23.

system and is listed in Table 3. The ratio S_s/S_D, i.e., $(k_s/k_D)^{1/3}$, is plotted against M_w in Figure 8C. The value is larger than 1.3 and increases with decreasing M_w. S_s/S_D is thus larger than S_T/S_D in all the M_w studied, indicating that the hydrodynamic two-body interactions represented by S_s are effective over longer distances than the thermodynamic/hydrodynamic two-body interactions, S_D.

Second Concentration-Dependent Coefficients. In Figure 11, the present k_{D2} data, which are negative, are plotted against M_w. The points fall on line 1, represented by

$$k_{D2} = -1.40 \times 10^{-6} M_w^{1.54} \text{ (cm}^6 \text{ g}^{-2}\text{)} \qquad (24)$$

The slope of 1.54 is slightly smaller than 1.60, predicted from $k_{D2} \propto (A_2 M_w)^2$ for linear flexible polymers in the good-solvent limit. The k_{s2} data are shown on line 2 in the same figure. They are fitted, over the whole range of M_w, by

$$k_{s2} = -6.93 \times 10^{-6} M_w^{1.48} \text{ (cm}^6 \text{ g}^{-2}\text{)} \qquad (25)$$

However, the exponent of M_w, 1.48, is slightly smaller than that of k_{D2}.

Figure 12A shows the volume-fraction frame k_{D2} and k_{s2} values, i.e., k_{D2}^V and k_{s2}^V, as a function of X for the present system. They depend strongly on X: Each decreases with increasing thermodynamic interactions of the chains, X, with $|k_{D2}^V| < |k_{s2}^V|$. The k_{D2}^V and k_{s2}^V values of about −0.7 to −1.1 and −1.5 to −2.1, respectively, are much larger than the corresponding values, −11.53 and −21.47, predicted by Phillies for hard spheres.[15] Thus, well-swollen chains should not be described by the hard sphere approximation, but more care must be taken of the hydrodynamic interactions between the chains.

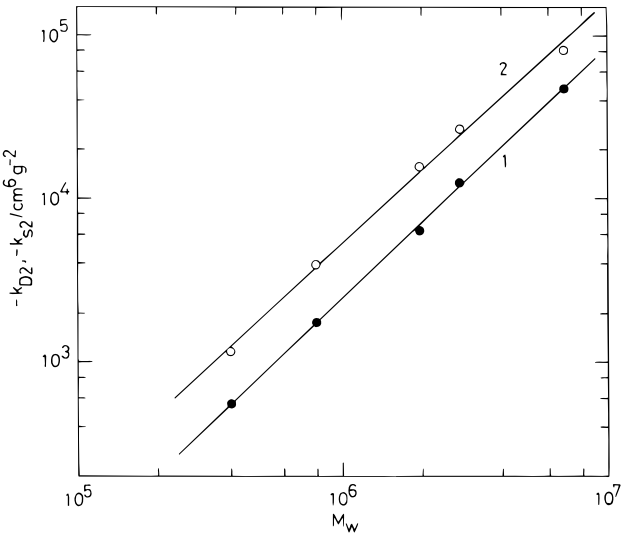

Figure 11. Molecular weight dependence of k_{D2} and k_{s2} for poly(α-methylstyrene) in benzene at 30 °C: (●) k_{D2} and (○) k_{s2}. The solid lines 1 and 2 represent eqs 24 and 25, respectively.

The sum $k_{D2}^V + k_{s2}^V$ is plotted against X in Figure 12B. The points are located on the curve represented by

$$k_{D2}^V + k_{s2}^V = 48gX^6 - 6X^4(8X - 6) \qquad (26)$$

with a fitting constant $g = 0.22-0.23$. Equation 26 is obtained by applying the Akcasu and Benmouna relations,[21] $k_D^V = X^2(8X - 6)$ and $k_s^V = 6X^2$, to the thermodynamic one, $k_{D2} + k_{s2} + k_D k_s = 3A_2 M_w$ (eq 8), with $g = A_3/A_2^2 M_w$. The fitted value of $g = 0.22-0.23$ is found to be in complete agreement with the experimental value 0.228, which will later be reported for the present PαMS−benzene system for $3 \times 10^5 < M_w < 10^7$.[32] In the same figure, a $k_{D2}^V + k_{s2}^V$ curve for larger g, e.g., $g = 1/3$, is shown. This g value is within the range $g = 0.25-0.49$, reported recently for polystyrene in benzene.[22,23] The curve is however far above the data points and not sufficient to explain the present results.

By analogy of the thermodynamic g factor, $g = A_3/A_2^2 M_w$, mentioned above, we define here the hydrodynamic g factors by $g_D = k_{D2}^V/k_D^{V\,2} = k_{D2}/k_D^2$ and $g_s = k_{s2}^V/k_s^{V\,2} = k_{s2}/k_s^2$ for the concentration coefficients of diffusion and sedimentation, respectively. The g_D and g_s values were calculated for the present system, as summarized in Table 3, and are plotted against M_w in Figure 13. They are both negative; g_D is −0.14 over all the M_w studied, while g_s first increases in its absolute value and then reaches a constant of −0.05 with increasing M_w. Apparently, the independence of g_D with M_w is consistent with the behavior of linear flexible polymers under the hard sphere approximation. However, this consistency is attributable to an occasional cancellation of the molecular weight dependences of k_D and k_{D2}, which do not fulfill the behavior in the good-

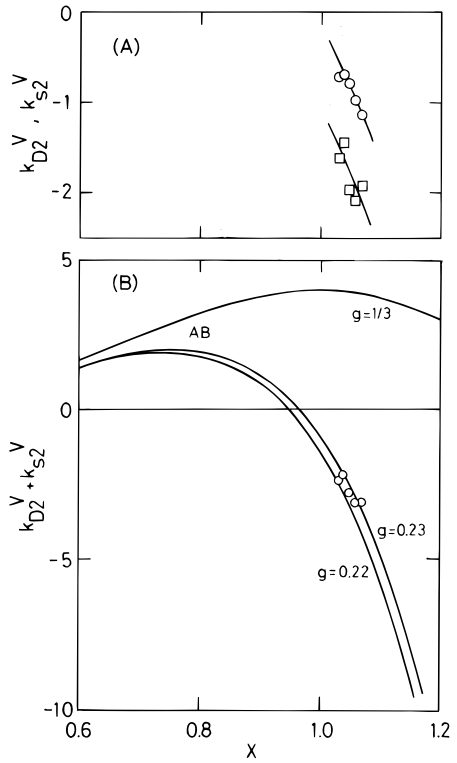

Figure 12. Variation of the volume-fraction frame k_{D2} and k_{s2} values, i.e., k_{D2}^V and k_{s2}^V, with X for poly(α-methylstyrene) in benzene at 30 °C: (A) (○) k_{D2}^V vs X plot, (□) k_{s2}^V vs X plot and (B) $k_{D2}^V + k_{s2}^V$ vs X plot. The solid lines AB represent the thermodynamic equation obtained from the Akcasu and Benmouna relation, $k_{D2}^V + k_{s2}^V = 48gX^6 - 6X^4(8X - 6)$ (eq 26), with three different g values which are defined thermodynamically by $g = A_3/A_2^2M_w$.

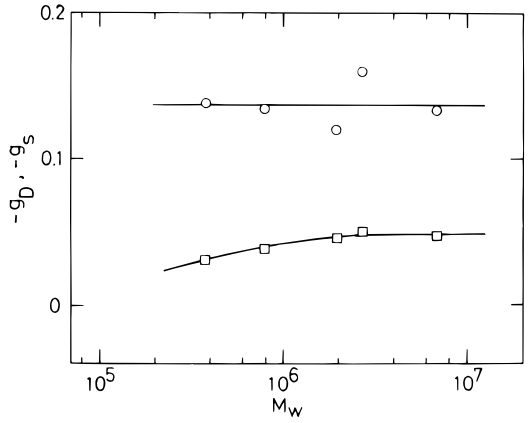

Figure 13. Molecular weight dependence of hydrodynamic g factors, g_D and g_s, defined by $g_D = k_{D2}/k_D^2$ and $g_s = k_{s2}/k_s^2$, for poly(α-methylstyrene) in benzene at 30 °C: (○) g_D and (□) g_s.

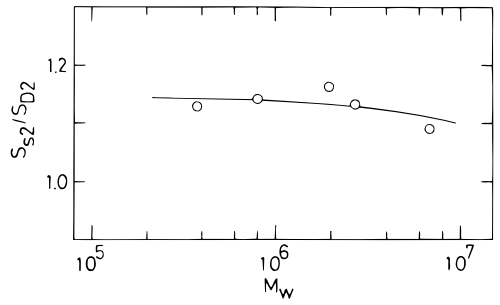

Figure 14. Ratio of the hydrodynamic three-body interaction radii, S_{s2}/S_{D2}, plotted against the molecular weight for poly(α-methylstyrene) in benzene at 30 °C.

solvent limit, as already described. The g_D value of −0.14 is indeed inconsistent with −5.48, predicted by Phillies for hard spheres.[15] The increase of $|g_s|$ with M_w reflects the molecular weight dependence of k_s (eq 23) which is much smaller than for hard spheres, $k_s \propto M_w^{0.80}$. The asymptote g_s of −0.05 at higher M_w thus disagrees with the corresponding value of −0.346 by Phillies.[15]

In Figure 14 is plotted against M_w the ratio of the hydrodynamic three-body interaction radii for the present study, S_{s2}/S_{D2}. Here S_{D2} and S_{s2} are defined as the effective radius which represents k_{D2} and k_{s2}, respectively, by the relations:

$$k_{D2} = [4(4\pi N_A {S_{D2}}^3/3M_w)]^2,\ k_{s2} = [(4(4\pi N_A {S_{s2}}^3/3M_w)]^2 \quad (27)$$

We call S_{D2} and S_{s2} the k_{D2} and k_{s2} radius, respectively, and the values are summarized in Table 3. The ratio S_{s2}/S_{D2} decreases gradually with increasing M_w, but the value is never below 1.1, indicating that the purely hydrodynamic three-body interactions, represented by the k_{s2} radius, are effective over a longer range than the interactions which concern the thermodynamic and hydrodynamic three-body radius, or the k_{D2} radius. This situation is the same as in the hydrodynamic two-body interactions where the k_s radius is larger than the k_D radius, as shown in Figure 8C.

In conclusion, k_D^V and k_s^V of poly(α-methylstyrene) in benzene are not constant (in contrast to the hard sphere approximation) but increase with increasing X, as predicted by Akcasu and Benmouna,[20,21] and $k_D^V + k_s^V$ obeys the Gibbs−Duhem relation $k_D^V + k_s^V = 8X^3$. k_{D2}^V and k_{s2}^V of poly(α-methylstyrene) in benzene are negative and decrease with increasing X, the sum $k_{D2}^V + k_{s2}^V$ being well represented by a thermodynamic relation combined with the k_D and k_s relations by Akcasu and Benmouna, $k_{D2}^V + k_{s2}^V = 48gX^6 - 6X^4(8X - 6)$, with $g = 0.22-0.23$. The hydrodynamic g_D factor is constant at −0.14 over the entire range of M_w ($3.8 \times 10^5 < M_w < 7 \times 10^6$) studied, while the g_s factor varies slightly with M_w at lower M_w but reaches an asymotote −0.05 for $M_w > 2 \times 10^6$. In addition, the ratios of the two-body hydrodynamic interactions, S_D/S_s, and the three-body ones, S_{D2}/S_{s2}, as well as the ratio of the hydrodynamic two-body radius to the thermodynamic one, S_D/S_T, are not equal to unity. Thus the hard sphere approximation fails to explain the hydrodynamic behavior of swollen chains in good solvents for poly(α-methylstyrene) in benzene.

References and Notes

(1) Nemoto, N.; Matika, Y.; Tsunashima, Y.; Kurata, M. *Macromolecules* **1984**, *20*, 425.
(2) Tsunashima, Y.; Nemoto, N. *Macromolecules* **1984**, *17*, 2931.
(3) Tsunashima, Y.; Hirata, M.; Nemoto, N.; Kurata, M. *Macromolecules* **1987**, *20*, 1992.
(4) Davidson, N. S.; Fetters, L. J.; Funk, W. G.; Hadjichristidis, N.; Graessley, W. W. *Macromolecules* **1987**, *20*, 2614.
(5) Lindner, J. S.; Wilson, W. W.; Mays, J. W. *Macromolecules* **1988**, *21*, 3304.
(6) Selser, J. C. *Macromolecules* **1981**, *14*, 1981. The molecular weights of the PαMS samples reported therein, which were determined with d*n*/d*c* = 0.108 mL/g for PαMS in toluene at 25 °C, were revised by using another d*n*/d*c* value, 0.122 mL/g, suggested by Lindner et al. (ref 5). The latter value is very close to 0.124 mL/g, newly reported by Cotts and Selser for PαMS in toluene at 25 °C (ref 8).
(7) Kim, S. H.; Ramsay, D. J.; Patterson, G. D.; Selser, J. C. *J. Polym. Sci., Polym. Phys. Ed.* **1990**, *11*, 222.
(8) Cotts, P. M.; Selser, J. C. *Macromolecules* **1990**, *23*, 2050.
(9) Sakato, M.; Kurata, M. *Polym. J.* **1970**, *1*, 260.

(10) Noda, I.; Saito, S.; Fujimoto, T.; Nagasawa, M. *J. Phys. Chem.* **1967**, *71*, 4048.
(11) Noda, I.; Mizutani, K.; Kato, T. *Macromolecules* **1977**, *10*, 618.
(12) Brown, W.; Zhou, P. *Macromolecules* **1991**, *24*, 5151.
(13) Fetters, L. J.; Hadjichristidis, N.; Lindner, J. S.; Mays, J. W.; Wilson, W. W. *Macromolecules* **1991**, *24*, 3127.
(14) Fetters, L. J.; Hadjichristidis, N.; Lindner, J. S.; Mays, J. W. *J. Phys. Chem. Ref. Data* **1994**, *23*, 619.
(15) Phillies, G. D. J. *J. Chem. Phys.* **1982**, *77*, 2623. Equations 4.11 and 4.12 in this reference have some errors. We revised them as follows: read 8.875 and 12.625 as 7.875 and 11.625, respectively, in eq 4.11, and read 0.875, 19.53, 4.625, and 51.74 as −0.125, 11.53, 3.625, and 43.74, respectively, in eq 4.12.
(16) Batchelor, G. R. *J. Fluid Mech.* **1972**, *52*, 245; **1976**, *74*, 1.
(17) Pyun, C. W.; Fixman, M. *J. Chem. Phys.* **1964**, *41*, 937.
(18) (a) Kops-Werkhoven, M. M.; Vrij, A.; Lekkerkerker, H. N. W. *J. Chem. Phys.* **1983**, *78*, 2760. (b) The second power in $(1 - \nu_2\rho_s)^2$ in eq 4 was given by Vink: Vink, H. J. *J. Chem. Soc., Faraday Trans.* **1985**, *81*, 1725. (c) The familiar but erroneous terms vanish: For example, the term $-\nu_2$ disappears in eq 7.
(19) Felderhof, B. U. *Physica A (Amsterdam)* **1977**, *89*, 373; *J. Phys. A.* **1978**, *11*, 929.
(20) Akcasu, A. Z.; Benmouna, M. *Macromolecules* **1978**, *11*, 1193.
(21) Akcasu, A. Z. *Polymer* **1981**, *22*, 1169.
(22) Nakamura, Y.; Norisuye, T.; Teramoto, A. *J. Polym. Sci., Polym. Phys. Ed.* **1991**, *29*, 153.
(23) Sato, T.; Norisuye, T.; Fujita, H. *J. Polym. Sci., Polym. Phys. Ed.* **1987**, *25*, 1.
(24) Kniewske, K. R.; Kulicke, W. H. *Makromol. Chem.* **1983**, *184*, 2173.
(25) Utiyama, H.; Tsunashima, Y.; Kurata, M. *J. Chem. Phys.* **1971**, *55*, 3133.
(26) Nemoto, N.; Tsunashima, Y.; Kurata, M. *Polymer J.* **1981**, *13*, 827.
(27) Tsunashima, Y.; Nemoto, N.; Kurata, M. *Macromolecules* **1983**, *16*, 584.
(28) Bawn, C. E. H.; Freeman, R. F.; Kamaliddin, A. R. *Trans. Faraday Soc.* **1950**, *46*, 862.
(29) Blair, J. E.; Williams, J. W. *J. Phys. Chem.* **1964**, *68*, 161.
(30) Li, J.; Wan, Y.; Xu, Z.; Mays, J. W. *Macromolecules* **1995**, *28*, 5347.
(31) Kato, T.; Miyaso, K.; Noda, I.; Fujimoto, T.; Nagasawa, M. *Macromolecules* **1970**, *3*, 777. The I and H fractions decrease, while the S fraction increases with decreasing M_w for $M_w < 2 \times 10^5$.
(32) Tsunashima, Y. Manuscript in preparation.
(33) Venkataswamy, K.; Jamieson, A. M.; Petschek, R. G. *Macromolecules* **1968**, *19*, 124.
(34) Benmouna, M.; Akcasu, A. Z. *Macromolecules* **1978**, *11*, 1187; **1980**, *13*, 409.
(35) Tsunashima, Y. *Macromolecules* **1988**, *21*, 2575.
(36) Shiwa, Y.; Tsunashima, Y. *Physica A* **1993**, *197*, 47.
(37) Tsunashima, Y. *Polym. J.* **1992**, *24*, 433.
(38) Douglas, J. F.; Freed, K. F. *Macromolecules* **1994**, *27*, 6088.
(39) s_0 data for PαMS in toluene at 25 °C by Noda et al. (refs 10 and 11) are fairly larger than the present ones for $M_w > 10^6$.
(40) A set of k_s^V and X values could be calculated only for the present data and ref 5. For others, however, we could not do anything for lack of D_0 or A_2 data.

MA951319K